Global analysis of differential luminal epithelial gene expression at mouse implantation sites

Ying Chen, Hua Ni, Xing-Hong Ma, Shi-Jun Hu, Li-Ming Luan, Gang Ren, Yue-Chao Zhao, Shi-Jie Li, Hong-Lu Diao, Xiu Xu, Zhen-Ao Zhao and **Zeng-Ming Yang**

College of Life Sciences, Northeast Agricultural University, Harbin 150030, China

(Requests for offprints should be addressed to Z-M Yang; Email: zmyang@neau.edu.cn)

Abstract

Although implantation types differ between species, the interaction between blastocyst trophectoderm and apical surface of the uterine epithelium is a common event during the implantation process. In this study, uterine luminal epithelium at implantation and inter-implantation sites was isolated by enzymatic digestion and used for microarray analysis. In a mouse microarray containing 12 345 unigenes, we found 136 genes upregulated more than twofold at the implantation site, while 223 genes were downregulated by at least twofold. Reverse transcription-PCR was used to verify the differential expression of seven upregulated and six downregulated genes chosen randomly from our microarray analysis, and the expression trends were similar. The differential expression patterns of eight upregulated genes were verified by *in situ* hybridization. Compared with the inter-implantation site on day 5 of pregnancy and the uterus on day 5 of pseudopregnancy, protease, serine, 12 neurotrypsin, endothelin-1, γ-glutamyl hydrolase, Ras homolog gene family, member U, T-cell immunoglobulin, and mucin domain containing 2, proline–serine–threonine phosphatase-interacting protein 2, 3-monooxgenase/tryptophan 5-monooxgenase activation protein, γ-polypeptide, and cysteine-rich protein 61 (*Cyr61*) were upregulated in the luminal epithelium at implantation site on day 5 of pregnancy. These genes may be related to embryo apposition and adhesion during embryo implantation. *Cyr61*, a gene upregulated at the implantation site, was chosen to examine its expression and regulation during the periimplantation period by *in situ* hybridization. *Cyr61* mRNA was specifically localized in the luminal epithelium surrounding the implanting blastocyst at day 4 midnight and on day 5 of pregnancy, and in the activated uterus, but not expressed in inter-implantation sites and under delayed implantation, suggesting a role for *Cyr61* in mediating embryonic–uterine dialog during embryo attachment. Our data could be a valuable source for future study on embryo implantation.

Journal of Molecular Endocrinology (2006) **37,** 147–161

Introduction

Although reproduction is critical to species survival, the process of achieving and maintaining pregnancy is relatively inefficient. Maximal fecundity, the probability of conception during one menstrual cycle, is approximately 30% (Zinaman *et al.* 1996). Impaired uterine receptivity is one of the major reasons for the failure of assisted reproductive techniques (Edwards 1995, Spandorfer & Rosenwaks 1999). Defects in implantation and trophoblast invasion are presently considered the major challenges for the establishment of pregnancy (Herrler *et al.* 2003).

Depending on the species, trophoblast penetration of the endometrium may remain superficial or continue deep into the endometrium. Nonetheless, all the implantation processes between species involve the interaction between the blastocyst trophectoderm and the apical surface of the uterine luminal epithelium (Carson *et al.* 2000). Normally, the apical surface of the luminal epithelium is non-adhesive. However, the uterine transition from pre-receptive to receptive requires fundamental structural and functional changes in epithelial cell organization (Kimber & Spanswick 2000), allowing for successful blastocyst attachment.

Implantation is a complex process involving spatiotemporally regulated endocrine, paracrine, autocrine, and juxtacrine modulators that span cell–cell and cell–matrix interactions. The successful implantation of an embryo depends upon cellular and molecular dialog between the uterus and the embryo (Dey *et al.* 2004). To date, although many specific factors have been identified during the implantation period, the molecular mechanism of embryo implantation is still unknown. Oligonucleotide microarray analysis has shed insight into a wide range of developmental, oncological, and pharmacological processes by allowing the simultaneous and quantitative assessment of expression levels of thousands of genes (Bethin *et al.* 2003). Recently, microarray analysis has been used to investigate temporal and spatial gene expression profiles in the mouse uterus during the implantation period (Yoshioka *et al.* 2000, Reese *et al.* 2001).

0952–5041/06/037–147
DOI: 10.1677/jme.1.02009
Online version via http://www.endocrinology-journals.org

However, whole uterine fragments were used in these studies. In the uterus, the luminal epithelium represents about 5–10%, the stroma 30–35%, and the myometrium 60–65% of the major uterine cell types (Finn & Porter 1975). It is difficult to characterize the specific gene expression in the luminal epithelium because of the interference from large amounts of uterine stroma and myometrium. Yoon *et al.* (2004) used laser capture microdissection (LCM) to isolate the luminal epithelium at implantation and inter-implantation sites for microarray analysis. Although luminal epithelium could be collected accurately by LCM, the mRNA count of luminal epithelium collected from frozen sections is very limited and needs to be amplified several times prior to microarray analysis. Because of the sensitivity in mRNA amplification, artificial errors could be a problem during data analysis. In this study, we used enzymatic digestion to isolate luminal epithelium from the mouse uterus at implantation and inter-implantation sites, of over 100 mice. The luminal epithelium obtained by this method was directly used for mRNA extraction and microarray analysis without any amplification. Differential gene expression profile in uterine luminal epithelium at implantation site was performed using a mouse microarray containing 12 345 unigenes. Microarray data were confirmed by both reverse transcription (RT)-PCR and *in situ* hybridization.

Materials and methods

Animals and treatments

Mature mice (Kunming White outbred strain) were caged in a controlled environment with a ratio of 14 h light:10 h darkness cycle. All animal procedures were approved by the Institutional Animal Care and Use Committee of Northeast Agricultural University. Adult females were mated with fertile or vasectomized males of the same strain to induce pregnancy or pseudopregnancy respectively (day 1 = day of vaginal plug). Pregnancy on days 1–4 was confirmed by recovering embryos from the reproductive tracts. The implantation sites on the day 4 midnight (2400 h) and on day 5 were identified by i.v. injection of 0·1 ml 1% Chicago blue (Sigma) in 0·85% sodium chloride.

To induce delayed implantation, pregnant mice were ovariectomized under ether anesthesia between 0830 and 0900 h on day 4 of pregnancy. Progesterone (1 mg/mouse) was injected to maintain delayed implantation, from days 5 to 7. Estradiol-17β (25 ng/mouse) was given to progesterone-primed delayed-implantation mice to terminate delayed implantation. The mice were sacrificed to collect uteri 24 h after estrogen treatment. Implantation sites were identified by i.v. injection of Chicago blue solution. Delayed implantation was confirmed by flushing the blastocysts from one horn of the uterus.

Hormonal treatments were initiated 2 weeks after mature female mice were ovariectomized. Controls received 0·1 ml of sesame oil per mouse. For hormonal treatments, the ovariectomized mice were treated with an injection of estradiol-17β (100 ng/mouse; Sigma), progesterone (1 mg/mouse; Sigma), or a combination of the same doses of progesterone and estradiol-17β for 24 h. All steroids were dissolved in sesame oil and injected subcutaneously.

Isolation of uterine luminal epithelium

Pregnant mice on day 5 (0800–0830 h) of pregnancy were used to collect implantation and inter-implantation sites by tail vein injection of Chicago sky blue. For microarray analysis, the uterine fragments with the strongest blue staining on day 5 of pregnancy were collected for implantation sites, and the blue dye-free areas between implantation sites for inter-implantation sites.

Luminal epithelium of mouse uterus was isolated as previously described (Bigsby *et al.* 1986, Tan *et al.* 2004) and slightly modified. Uteri at implantation and inter-implantation sites were split longitudinally and incubated in 5 ml 1% (w/v) trypsin and 6 mg/ml dispase in HBSS solution (Gibco) at 4 °C for 1 h, 20 °C for 1 h, and 37 °C for 10 min respectively. After brief shaking, luminal epithelial cells were collected from the supernatants with a mouth-controlled pipette under a stereomicroscope. After enzymatic digestion, implanted blastocysts were found in the digestion solution. To avoid the contamination of glandular epithelium, detached blastocysts, and suspended cells, only the pieces in a single layer were collected. In order to remove any attached uterine stromal cells, the supernatants were centrifuged for 5 min at 200 ***g***. Then the cell pellets were resuspended in HBSS and spun twice. Finally, the pellets containing uterine luminal epithelial cells were pooled for RNA extraction with TRIZOL reagent (Sigma).

To examine the purity of isolated uterine luminal epithelial cells, an aliquot of cell pellets prior to RNA extraction was resuspended in DMEM/F12 medium (1:1; Sigma) with 10% (v/v) fetal bovine serum (Gibco) and plated on a 35 mm culture dish. After the cells reached around 80% confluence, they were washed three times in PBS and fixed in cold methanol for 10 min. The cells were blocked with 1% (w/v) BSA in PBS for 1 h and incubated in goat anti-cytokeratin antibody (Santa Cruz Biotechnology, Inc., Santa Cruz, CA, USA) at 4 °C overnight. After washing three times in PBS, the cells were incubated with biotinylated rabbit anti-goat IgG at 37 °C for 30 min and straptavidin conjugated with alkaline phosphatase for 30 min, followed by three washes in PBS. The cells were then

incubated in Vector Red substrate (Vector Laboratories, Burlingame, CA, USA). Positive reaction products were indicated by red color. Based on cytokeratin immunostaining, the purity of the uterine luminal epithelial cells was approximately 99%.

Microarray analysis

Uterine luminal epithelium was isolated from implantation and inter-implantation sites as described above respectively. More than 100 mice were used for this study. After uterine luminal epithelium were isolated and extracted for RNA with TRIZOL reagent, reverse transcription, probe labeling, and hybridization were performed according to the procedures from Biostar Biotech, Inc. (Shanghai, China). Briefly, RNA samples extracted with TRIZOL reagent were labeled with Cy3 or Cy5 by direct incorporation of Cy3-dUTP or Cy5-dUTP in the reverse transcription reaction, i.e. Cy3 for inter-implantation sites and Cy5 for implantation sites. Labeled samples from implantation and inter-implantation sites were co-hybridized with Genechip BiostarM-141s containing 12 345 unigenes with defined functions (Biostar Biotech, Inc.). After hybridization at 42 °C for 16 h, the genechip was washed and air-dried. The fluorescent intensities of Cy3 and Cy5 were scanned with ScanArray 4000 (Packard Bioscience, Billerica, MA, USA) and analyzed with GenePix Pro 3.0 software (Axon Instruments, Foster City, CA, USA). The genes having Cy5:Cy3 ratio within 0·1–10 were chosen for further analysis. In order to eliminate the systematic variation, the Cy3 value of each gene was normalized using a normalization factor (0·976), which was the mean value of $\log_2$(Cy5 intensity/Cy3 intensity). The ratio of each gene expression was calculated as Cy5 intensity over normalized Cy3 intensity. The criterion of twofold difference was used to choose the up- and downregulated genes for the following analysis as described previously (Yang *et al.* 2002).

RT-PCR

RNA was extracted from isolated luminal epithelium of both implantation and inter-implantation sites, using TRIZOL reagent. RNA samples were then treated with RQ1 DNase I (Promega) to remove any genomic DNA contamination, extracted with phenol/chloroform, precipitated, and dissolved in formamide at a final concentration of 1 μg/μl and stored at −70 °C.

Total RNAs were reverse-transcribed in a reaction volume of 20 μl containing 22 units of RT and 2·5 μM oligo-dT using a BcaBEST RNA PCR kit (Takara Biotechniques, Dalian, China). The intensity of amplified bands was scanned with UVP Laboratory Imaging and Analysis System (UVP, Inc., Upland, CA, USA). Primers, annealing temperatures, and expected product sizes for these genes are listed in Table 1. Band densities for each gene were normalized to glyceraldehyde-3-phosphate dehydrogenase (*Gapdh*) expression and the ratios determined. The amplification cycle number of each gene was chosen based on our previous tests to ensure that the amplification was terminated during the exponent phase. RT-PCR for each gene was repeated on, at least, three different samples. The RT-PCR product of each gene was verified by sequencing. Statistical analysis was performed with SPSS software (SPSS Inc., Chicago, IL, USA).

In situ hybridization

Total RNAs from pregnant mouse uteri were reverse-transcribed and amplified with the corresponding primers for each gene listed in Table 1. The amplified fragment of each gene was recovered from agarose gel and cloned into pGEM-T plasmid (pGEM-T Vector System 1l; Promega). The cloned fragments were further verified by sequencing. The recombinant plasmid was amplified individually with the primers for T7 and SP6 to prepare templates for labeling sense or antisense probe respectively. Digoxigenin (DIG)-labeled antisense or sense cRNA probe was transcribed *in vitro* using a DIG RNA labeling kit (Roche).

Uteri were cut into 4–6 mm pieces and flash frozen in liquid nitrogen. Frozen sections (10 μm) were mounted on 3-aminopropyltriethoxy silane (Sigma)-coated slides and fixed in 4% paraformaldehyde solution in PBS. The sections were washed twice in PBS, treated in 1% Triton-100 for 20 min, and again washed three times in PBS. Following pre-hybridization in the 50% formamide/5× SSC solution (1× SSC is 0·15 M sodium chloride, 0·015 M sodium citrate) at room temperature for 15 min, the sections were hybridized as previously described (Ni *et al.* 2002). Endogenous alkaline phosphatase activity was inhibited with 2 mM levamisole (Sigma). All the sections were counter-stained with 1% methyl green. The positive signal was visualized as a dark brown color. *In situ* hybridization for each gene was repeated at least three times with the uteri from three different animals at each stage.

Results

Microarray analysis

In order to examine the differential gene expression profile in uterine luminal epithelium on day 5 of pregnancy in the mouse, luminal epithelium was isolated from uterine stroma, glandular epithelium, myometrium, and serosa by enzymatic digestion on day 5 of pregnancy at implantation or inter-implantation

Table 1 Primer sequences and anticipated product lengths used for reverse transcriptase (RT)-PCR and *in situ* hybridization

Gene	Accession number	Primer pair	Size (bp)	Cycles
Protease, serine, 12 neurotrypsin (*Prss12*; motopsin)	NM_008939	CTATGCAGTTCGAGTTGG CTTTGACTCCACATCCATAC	500	33
Gap junction membrane channel protein β 6 (*Gjb6*)	BC016507	AATGACTGGCCTTCCTTAC GAAGCAACAGGGTCAAGC	305	35
Phospholipase A_2 group VII (platelet-activating factor acetylhydrolase, plasma; *Pla2g7*)	NM_013737	GGTTCAGCAAAGAGCAATAG ATGGCTACTCTGGAATCG	480	32
Endothelin 1 (*Edn1*)	NM_010104	CAGTTAGATGTCAGTGCG AAGTCCTCTGTCATTCCC	549	35
Mouse cysteine rich protein 61 (*Cyr61*)	NM_010516	CAGCAAGACCAAGAAATC CCTGAACTTGTGGATGTC	283	33
Inhibitor of DNA-binding 3 (*Idb3*)	NM_008321	TGCTACGAGGCGGTGTGCTG AGTGAGCTCAGCTGTCTGGATCGG	288	30
Mouse complement component factor h (*Cfh*)	NM_009888	CTATGTGAAGTTGTGAAGTGTC CAGTTACAGGATAGAAGCC	490	35
N-Acetylneuraminate pyruvate lyase (*Npl*)	NM_028749	AAAGATGCCCTGATAAGC CTCTGGATACGAAACTGG	392	35
Brain acyl-CoA hydrolase (*Bach*)	NM_133348	AATGTGGCTGGCAATGTTC ATAGCGTTTCCGACCCTC	387	35
Solute carrier family 6 (neurotransmitter transporter, taurine), member 6 (*Slc6a6*)	NM_009320	CCTCCATCTGATCGCCTAG TGTGTGTGCGTGCATTTG	374	35
Myeloid differentiation primary response gene 88 (*Myd88*)	BC005591	CACGCACCTCAGTACACAC TAGAGAACGTGAAAGGAATAAG	522	33
Glutathione S-transferase, μ 2 (*Gstm2*)	BC037068	AGGATTACAAAGCCCAGAC CTTAGCTGCTTACTCTGAGG	316	31
Thymosin, β 4, X chromosome (*Tmsb4x*)	BC018286	GACAAACCCGATATGGCTG TCATCATCTCCCACCCAG	390	36
Glyceraldehyde-3-phosphate dehydrogenase (*Gapdh*)	M32599	ACCACAGTCCATGCCATCAC TCCACCACCCTGTTGCTGTA	452	22
γ-Glutamyl hydrolase (*Ggh*)	NM_010281	GAGTTATTGGATTCATTAGC GTGGTGACTGTTCTTCCG	318	35
Ras homolog gene family, member U (*Rhou*)	NM_133955	GCCTGACTCTCGCAAATAG ACGCTTGCTCACTCTCAC	384	35
T-cell immunoglobulin and mucin domain containing 2 (*Timd2*)	BC028829	ATTTCCACGAGTCCACCAAC CTTCACATCTGGTCCGTTC	481	35
Proline–serine–threonine phosphatase-interacting protein 2 (*Pstpip2*)	NM_013831	AAGCAGCAAGTAGACAACG CATACATCTCGTCATTTGC	508	35
3-Monooxgenase/tryptophan 5-monooxgenase activation protein, γ-polypeptide (*Ywhag*)	BC008129	GGACGGCAACGAGAAGAAG GCCTTAGTTGTTGCCTTCAC	532	35

sites respectively. Figure 1 showed the structure of mouse uterus on day 5 of pregnancy at implantation site stained with hematoxylin and eosin, showing that the blastocyst was already attached on the luminal epithelium, which was still intact at the implantation site. During enzymatic digestion, the implanting blastocysts were detached from luminal epithelium, since the blastocysts were already found in the digestion solution. Additionally, a single layer of luminal epithelium was collected with a mouth-controlled pipette under a stereomicroscope to avoid the contamination of blastocysts, stromal cells, and glandular epithelium during the enzymatic digestion.

The differential gene expression profile in the luminal epithelium isolated from mouse uteri between implantation and inter-implantation sites was analyzed by a microarray containing 12 345 unigenes. Totally 136 genes were upregulated and 223 genes downregulated by at least twofold in implantation site compared with the inter-implantation site. The up- and downregulated genes with known functions are listed in Tables 2 and 3 respectively. Among the upregulated genes, 24 were upregulated by at least threefold, with protease, serine, 12 neurotrypsin (*Prss12*) being the most dramatically upregulated gene (6·75-fold). *Prss12*, also called motopsin, was highly expressed in the mouse brain (Iijima *et al.* 1999). Only 27 genes were downregulated by at least threefold. The highest change among downregulated genes with known function was *N*-acetylneuraminate pyruvate lyase (*Npl*) by 5·26-fold.

Among the significantly upregulated genes, most genes had functions related to catalytic activity (19·2%), protein binding (12·0%), nucleic acid binding (8·8%),

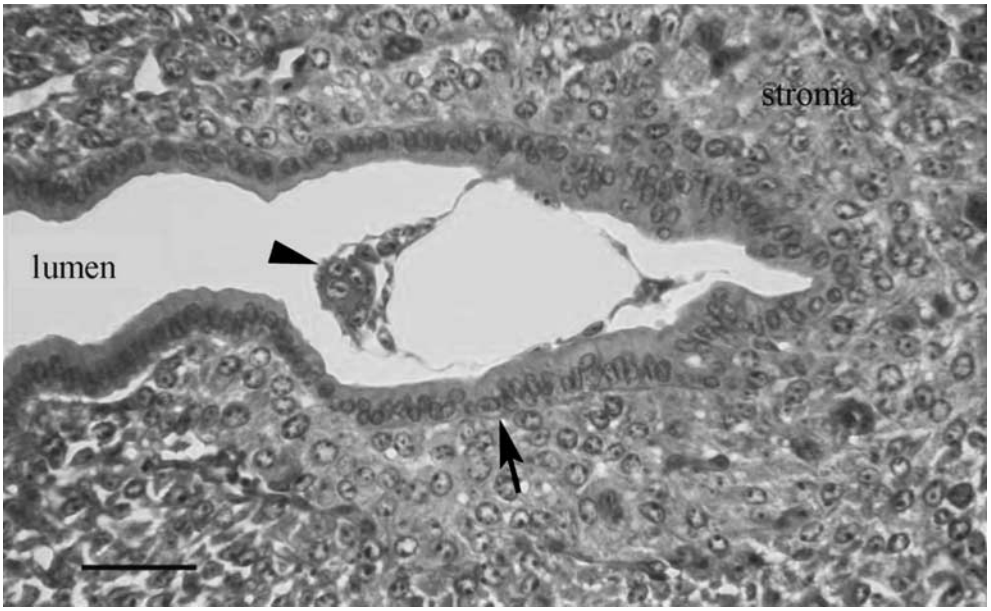

Figure 1 A hematoxylin–eosin staining of mouse uterus at implantation site on day 5 of pregnancy, showing that the blastocyst attached on the luminal epithelium. Arrow: luminal epithelium; arrowhead: blastocyst; bar = 25 μm.

transporter activity (7·2%), and hydrolase activity (6·4%). Based on the molecular functions, the percentages and categories of the downregulated genes were similar to that of upregulated genes. According to the categories of biological processes, both up- and downregulated genes are mainly related to metabolism, cell communication, cell growth and/or maintenance, signal transduction, and transport. There are no significant differences among the up- and downregulated genes. Nevertheless, 5·6% (seven genes) of the upregulated genes are related to cell adhesion, whereas only 1·7% (three genes) of the downregulated genes were related to cell adhesion. Furthermore, 3·2% (four genes) of the upregulated genes were involved in blood vessel development, while none of the downregulated genes were related to this function. After these genes were classified according to cellular components, 24·0% (30 genes) of the upregulated genes were extracellular components, whereas 8·7% (15 genes) of the downregulated genes were related to this function.

Confirmation by RT-PCR

To verify the data from microarray analysis, we randomly chose seven upregulated and six downregulated genes to examine their expression patterns by semi-quantitative RT-PCR. After the expression of each gene was normalized to *Gapdh* expression, the ratio between implantation and inter-implantation sites showed similar expression trends from both RT-PCR and microarray analysis, but the expression ratio between them did not completely match between RT-PCR and microarray analysis (Fig. 2). The ratio from microarray analysis was slightly higher than that from RT-PCR except for *Npl*, which was decreased by 5·26-fold, in microarray, but 6·66 in RT-PCR.

Confirmation by *in situ* hybridization

In order to further verify the microarray data, seven upregulated genes were randomly chosen to examine their expression on day 5 of pregnancy and pseudopregnancy by *in situ* hybridization. Compared with the inter-implantation site on the day of pregnancy and the uterus on day 5 of pseudopregnancy, all of these seven genes were upregulated in the luminal epithelium at implantation site on day 5 of pregnancy (Fig. 3). However, their expression patterns were slightly different. *Prss12* was strongly expressed in the glandular epithelium and the luminal epithelium near the blastocyst (Fig. 3A). Endothelin-1 (*Edn1*) is a 21-amino acid vasoconstrictor peptide originally isolated from endothelial cells (Rubanyi & Polakoff 1994). *Edn1* was highly detected in the luminal epithelium surrounding the implanting blastocyst (Fig. 3D). γ-Glutamyl hydrolase (*Ggh*), a lysosomal endopeptidase, was identified as a biomarker for pulmonary neuroendocrine tumors (He *et al.* 2004). *Ggh* was strongly expressed in all the luminal epithelium

Table 2 Genes upregulated by at least twofold at implantation sites

Description	Accession	Fold	Function
Prss12	NM_008939	6·75	Chymotrypsin activity
Gjb6	BC016507	6·15	Connexon channel activity
Pla2g7	NM_013737	4·80	1-Alkyl-2-acetylglycerophosphocholine esterase activity
Insulin-like growth factor-binding protein 4 (*Igfbp4*)	BC019836	4·36	Insulin-like growth factor-binding; receptor activity
Edn1	NM_010104	4·05	Toxin activity
Mouse *Cyr61*	NM_010516	3·78	Cell adhesion molecule
Fibrinogen A α polypeptide	BC005467	3·56	Unspecified
Secretory leukocyte protease inhibitor (*Slpi*)	NM_011414	3·53	Peptidase activity
Kininogen (*Kng*)	NM_023125	3·48	Cysteine protease inhibitor
Idb3	NM_008321	3·33	Transcription corepressor
Cerebellum postnatal development associated protein 2 (*Cadps2*)	AF000969	3·32	Protein binding
Growth differentiation factor 15 (*Gdf15*)	NM_011819	3·24	Growth factor activity
Ywhag	BC008129	3·12	Protein kinase C binding
Secreted acidic cysteine-rich glycoprotein (*Sparc*)	NM_009242	3·08	Calcium ion binding
Fatty acid desaturase 2 (*Fads2*)	NM_019699	2·99	Stearoyl-CoA 9-desaturase activity
Kruppel-like factor 4 (gut; *Klf4*)	NM_010637	2·90	Transcription factor activity
N-myc downstream regulated 1 (*Ndr1*)	NM_010884	2·84	Unspecified
Glutaredoxin 1 (thioltransferase; *Glrx1*)	NM_053108	2·78	Electron transporter activity
S100 calcium-binding protein A6 (calcyclin; *S100a6*)	NM_011313	2·59	Calcium ion binding
Partial mRNA for putative F-box protein 4 (*Fbx4*)	AJ300659	2·58	Unspecified
Neural cell adhesion molecule 1	X15052	2·56	Cell adhesion molecule
Extracellular matrix protein 1 (*Ecm1*)	NM_007899	2·49	Carrier activity
Gap junction membrane channel protein β 1 (*Gjb1*)	NM_008124	2·47	Connexon channel activity
Potassium intermediate/small conductance calcium-activated channel, subfamily N, member 2 (*Kcnn2*)	NM_080465	2·45	Calmodulin binding
γ-Glutamyl hydrolase (*Ggh*)	NM_010281	2·44	γ-Glutamyl hydrolase
Pla2g7	NM_013737	2·39	1-Alkyl-2-acetylglycerophosphocholine esterase activity
Nicolin 1 (*Nicn1*)	NM_025449	2·39	Unspecified
Small proline-rich protein 2I (*Sprr2i*)	NM_011475	2·39	Structural molecule activity
Poly(A) polymerase III	U52197	2·38	RNA binding
Thrombopoietin (*Thpo*)	NM_009379	2·38	Cytokine activity
Microsomal glutathione S-transferase 1 (*Mgst1*)	NM_019946	2·36	Glutathione transferase activity
Wingless-related MMTV integration site 7B (*Wnt7b*)	NM_009528	2·33	Receptor binding
Ribonuclease 1, pancreatic (*Rib1*)	NM_011271	2·33	Nucleic acid binding
TAF12 RNA polymerase II, TATA box-binding protein (TBP)-associated factor, 20 kDa (*Taf12*)	NM_025579	2·33	DNA binding
Aldehyde dehydrogenase (ALDH3B1)	AF362571	2·29	Oxidoreductase activity
Tangerin (LOC114601)	NM_053252	2·27	Actin binding
Timd2	BC028829	2·26	Unspecified
Gap junction membrane channel protein α 5 (*Gja5*)	NM_008121	2·25	Connexon channel activity
Sorting nexin 2 (*Snx2*)	NM_026386	2·21	Protein transporter activity
Hypothetical protein BC005730 (LOC230822)	NM_145555	2·21	Unspecified
Proprotein convertase subtilisin/kexin type 5	D17583	2·19	Subtilase activity
Histidine ammonia lyase (*Hal*)	NM_010401	2·18	Ammonia ligase activity
Fatty acid desaturase 3 (*Fads3*)	NM_021890	2·15	Oxidoreductase activity
Catenin α 2 (*Catna2*)	NM_009819	2·15	Cell adhesion molecule
Glucose-6-phosphatase, transport protein 1 (*G6pt1*)	NM_008063	2·14	Sugar porter activity
Purine-nucleoside phosphorylase (*Pnp*)	NM_013632	2·13	Phosphorylase activity
Pyruvate kinase liver and red blood cell (*Pklr*)	NM_013631	2·13	Magnesium ion binding
Rhou	NM_133955	2·12	GTP binding
Neuroblastoma, suppression of tumorigenicity 1 (*Nbl1*)	NM_008675	2·12	Unspecified
B-cell translocation gene 3 (*Btg3*)	NM_009770	2·11	Transcription factor activity
Pstpip2	NM_013831	2·11	Actin binding
Sulfide quinone reductase-like (yeast; *Sqrdl*)	NM_021507	2·10	Disulfide oxidoreductase activity
Angiogenin (*Ang*)	NM_007447	2·09	Nucleic acid binding
Serine (or cysteine) proteinase inhibitor, clade H (heat shock protein 47), member 1 (*Serpinh1*)	NM_009825	2·09	Heat shock protein activity

(continued)

Table 2 *Continued*

Description	Accession	Fold	Function
Mgst1	NM_019946	2·07	Glutathione transferase activity
Actin-related protein 8 homolog (*S. cerevisiae*; *Actr8*)	NM_027493	2·07	Structural constituent of cytoskeleton
Tubby like protein 4 (*Tulp4*)	NM_054040	2·06	Unspecified
Degenerative spermatocyte homolog (Drosophila; *Degs*)	NM_007853	2·05	Metallopeptidase activity
Cfh	NM_009888	2·05	Complement activity
Guanosine monophosphate reductase (*Gmpr*)	NM_025508	2·02	GMP reductase activity
N-Deacetylase/*N*-sulfotransferase (heparin glucosaminyl) 4 (*Ndst4*)	NM_022565	2·01	Sulfotransferase activity
V-abl Abelson murine leukemia oncogene 1	J02995	2·01	ATP binding
Malic enzyme, supernatant (*Mod1*)	NM_008615	2·01	Malate dehydrogenase (decarboxylating) activity
Syndecan 1 (*Sdc1*)	NM_011519	2·00	Cytoskeletal protein binding
Protein kinase C and casein kinase substrate in neurons 2 (*Pacsin2*)	NM_011862	2·00	Cytoskeletal protein binding
Nucleosome-binding protein 1 (*Nsbp1*)	NM_016710	2·00	Chromatin binding

except for that surrounding the implanting blastocyst (Fig. 3G). A low level of *Ggh* expression was also seen in the luminal epithelium at inter-implantation site (Fig. 3H), but not in day 5 pseudopregnant uterus (Fig. 3I). Ras homolog gene family member U (Rhou; Santin *et al.* 2005) was detected in both luminal epithelium and subluminal stromal cells on day 5 of pregnancy at implantation site (Fig. 3J), but not at inter-implantation site on day 5 of pregnancy (Fig. 3K), and on day 5 of pseudopregnancy (Fig. 3L). T-cell immunoglobulin and mucin domain containing 2 (*Timd2*) is critical for the regulation of Th2 responses during autoimmune inflammation (Chakravarti *et al.* 2005). *Timd2* was detected mainly in the luminal epithelium surrounding the implanting blastocyst (Fig. 3M). Proline–serine–threonine phosphatase-interacting protein 2 (*Pstpip2*) regulates F-actin bundling, and enhances filopodia formation and motility in macrophages (Chitu *et al.* 2005). A low level of *Pstpip2* expression was observed in all the luminal epithelium at implantation site (Fig. 3P). 3-Monooxgenase/tryptophan 5-monooxgenase-activation protein, γ-polypeptide (*Ywhag*), also called 14-3-3 γ, is a member of 14-3-3 family (Takahashi 2003). *Ywhag* expression was strongly detected in the luminal epithelium surrounding the implanting blastocyst and weakly in the subluminal stromal cells (Fig. 3S).

Expression and regulation of cysteine-rich protein 61 (*Cyr61*) in mouse uterus

In our microarray analysis, *Cyr61* was upregulated by 3·77 at the implantation site. *Cyr61* is also known as CCN1 (CCN is the initial of *Cyr61*, connective tissue growth factor (*Ctgf*), and nephroblastoma-overexpressed, NOV) and belongs to the CCN family (Perbal 2001). Because *Cyr61* was highly expressed in human endometrium and upregulated in the endometria of women with endometriosis (Absenger *et al.* 2004, Punyadeera *et al.* 2005), *Cyr61* was then chosen to verify the expression pattern and to examine its expression during early pregnancy, pseudopregnancy, delayed implantation, and steroid hormonal treatments by *in situ* hybridization. There was no detectable *Cyr61* expression in the uterus from days 1 to 3 of pregnancy (data not shown). *Cyr61* expression was not detected in the mouse uterus on the morning of day 4 of pregnancy (Fig. 4A), whereas it was observed in the luminal epithelium immediately surrounding the blastocyst on day 4 midnight when the attachment reaction was just initiated (Fig. 4B). On day 5 of pregnancy, when embryo implantation occurred, *Cyr61* mRNA signals were seen only in the luminal epithelium of mouse uterus at the implantation site (Fig. 4C), but not at the inter-implantation site (Fig. 4D). Furthermore, *Cyr61* signals were not detected in the mouse uterus on day 5 of pseudopregnancy (Fig. 4E) or during delayed implantation (Fig. 4G). After delayed implantation was terminated by estrogen treatment and the embryos implanted, *Cyr61* mRNA expression was once again observed in the luminal epithelium (Fig. 4H), expression similar to that observed at the implantation sites on day 5 of pregnancy. After *Cyr61* anti-sense probe was replaced with *Cyr61* sense probe, there was no detectable signal in the uterus on day 5 of pregnancy (Fig. 4F). Additionally, there was no detectable *Cyr61* mRNA signal in the uterus of ovariectomized mice. After ovariectomized mice were treated with either estrogen or progesterone for 24 h, Cyr61 mRNA expression was not seen in the uterus (data not shown).

Table 3 Genes downregulated by at least twofold at implantation sites

Description	Accession	Fold	Function
Npl	NM_028749	−5·26	*N*-Acetylneuraminate lyase activity
Calbindin-28K (*Calb1*)	NM_009788	−4·57	Calcium ion binding
Bach	NM_133348	−4·35	Palmitoyl-CoA hydrolase activity
Glutathione S-transferase, μ 1 (*Gstm1*)	NM_010358	−4·10	Glutathione transferase activity
Slc6a6	NM_009320	−3·85	β-Alanine transporter activity
Myd88	BC005591	−3·61	Transmembrane receptor activity
Interleukin 1 receptor, type I (*Il1r1*)	NM_008362	−3·38	Activating receptor activity
Neuronal differentiation related protein (*Ndrp*)	NM_031879	−3·14	Unspecified
Peripheral myelin protein, 22 kDa (*Pmp22*)	NM_008885	−3·08	Structural constituent of eye lens
ATPase, Ca^{++} transporting, plasma membrane 2 (*Atp2b2*)	NM_009723	−2·99	ATP binding
Sulfotransferase family 1A, phenol-preferring, member 1 (*Sult1a1*)	NM_133670	−2·99	Aryl sulfotransferase activity
Gstm2	NM_008183	−2·74	Glutathione transferase activity
Arylsulfatase A	X73230	−2·70	Cerebroside-sulfatase activity
Aldehyde dehydrogenase family 7, member A1 (*Aldh7a1*)	NM_138600	−2·70	Aldehyde dehydrogenase (NAD) activity
Progressive ankylosis (*Ank*)	NM_020332	−2·65	Inorganic diphosphate transporter activity
Son cell proliferation protein (*Son*)	NM_019973	−2·64	DNA binding
Tmsb4x	NM_021278	−2·61	Actin binding
ATP-binding cassette, subfamily G (WHITE), member 1 (*Abcg1*)	NM_009593	−2·54	ATP binding
Glutathione S-transferase, μ 6 (*Gstm6*)	NM_008184	−2·47	Glutathione transferase activity
Uracil DNA glycosylase (*Ung*)	NM_011677	−2·47	Uracil DNA *N*-glycosylase activity
Zmpste24	AY029194	−2·46	Metalloendopeptidase activity
Complement component 4-binding protein (*C4bp*)	NM_007576	−2·46	Complement activity
Syntaxin 18 (*Stx18*)	NM_026959	−2·43	Protein transporter activity
Low density lipoprotein receptor-related protein associated protein 1	D00622	−2·39	Heparin binding
Odd homeobox 1 protein (*Ob1*)	AF492703	−2·35	Transcriptional repressor activity
Interferon regulatory factor 1 (*Irf1*)	NM_008390	−2·33	Transcription factor activity
CGI-74-like SR-rich (LOC192196)	NM_138680	−2·29	Nucleic acid binding
Lymphocyte antigen 75 (*Ly75*)	NM_013825	−2·25	Receptor activity
Rho-associated coiled-coil forming kinase 2 (*Rock2*)	NM_009072	−2·23	ATP binding
Nucleolar protein 5 (*Nol5*)	NM_018868	−2·22	Chaperone activity
Tropomodulin 2 (*Tmod2*)	NM_016711	−2·18	F-actin capping activity
6-Pyruvoyl-tetrahydropterin synthase (*Pts*)	NM_011220	−2·17	Magnesium ion binding
α Glucosidase 2, α neutral subunit (*G2an*)	NM_008060	−2·16	Glucosidase activity
Creatine kinase, muscle (*Ckmm*)	NM_007710	−2·15	Creatine kinase activity
Duffy blood group (*Dfy*)	NM_010045	−2·15	Rhodopsin-like receptor activity
Endothelial differentiation, lysophosphatidic acid G-protein-coupled receptor 7 (*Edg7*)	NM_022983	−2·12	Lysosphingolipid and lysophosphatidic acid receptor activity
Phospholipid scramblase 1 (*Plscr1*)	NM_011636	−2·11	Calcium ion binding
Growth factor receptor bound protein 2 (*Grb2*)	NM_008163	−2·09	SH3/SH2 adaptor protein activity
Hypothetical protein (MGC27617)	NM_144813	−2·09	Calcium/potassium/sodium antiporter activity
Profilin 2 (*Pfn2*)	NM_019410	−2·08	Actin binding
Dihydrolipoamide branched chain transacylase E2 (*Dbt*)	NM_010022	−2·07	Acyltransferase activity
RAB4B, member RAS oncogene family (*Rab4b*)	NM_029391	−2·06	GTP binding
Survivor of motor neuron protein interacting protein 1 (*Sip1*)	NM_025656	−2·05	Pre-mRNA splicing factor activity
Creatine kinase, mitochondrial 1, ubiquitous (*Ckmt1*)	NM_009897	−2·05	Creatine kinase activity
Actinin α 3 (*Actn3*)	NM_013456	−2·05	Actin cross-linking activity
Glutathione S-transferase, α 4 (*Gsta4*)	NM_010357	−2·04	Glutathione transferase activity
Polymerase (DNA directed), δ 2, regulatory subunit (50 kDa; *Pold2*)	NM_008894	−2·03	DNA-directed DNA polymerase activity
Kruppel-type zinc finger protein KROX-25	AF281634	−2·02	DNA binding
Solute carrier family 15 (H+/peptide transporter), member 2 (*Slc15a2*)	NM_021301	−2·02	High-affinity oligopeptide transporter activity
Mitochondrial ribosomal protein L45 (*Mrpl45*)	NM_025927	−2·00	Structural constituent of ribosome

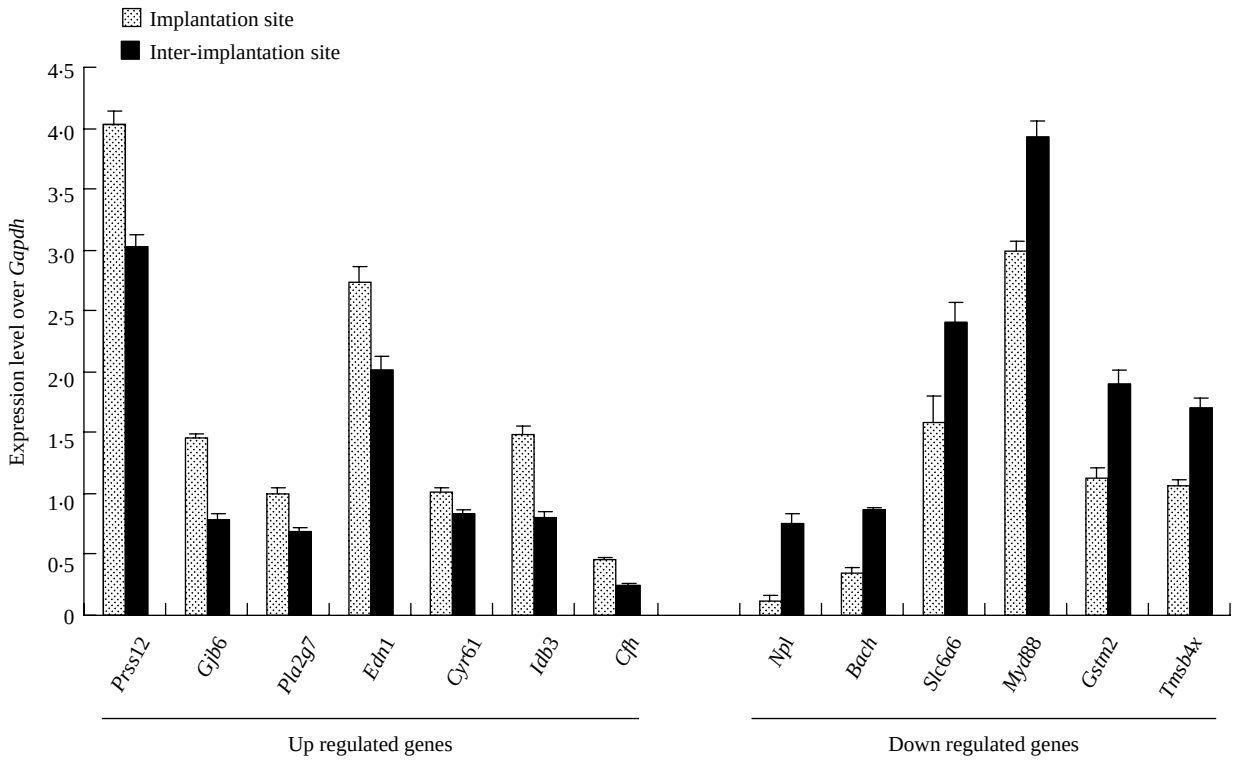

Figure 2 Semi-quantification of reverse transcriptase (RT)-PCR. RNA was extracted using TRIZOL reagent from isolated luminal epithelium on both implantation and inter-implantation sites respectively. To verify the data from microarray analysis, seven upregulated and six downregulated genes were randomly chosen to examine their expression patterns by semi-quantitative RT-PCR. After the expression of each gene was normalized to glyceraldehyde-3-phosphate dehydrogenase expression, the ratio of each gene between implantation site and inter-implantation site was determined. RT-PCR for each gene was repeated with three different samples. Values are presented as the mean ± S.E.M. (n=3).

Discussion

Embryo implantation is a process where the activated blastocyst establishes close contact with the uterine luminal epithelium and attaches to initiate implantation. However, the luminal epithelium represents only about 5–10% of uterine cell types (Finn & Porter 1975). Although implantation and inter-implantation sites can be distinguished by tail injection of Chicago blue dye solution (Psychoyos 1986), it is very hard to characterize the differential gene expression specifically in the luminal epithelium. Although luminal epithelium at implantation sites could be isolated using LCM, the samples obtained from LCM are very limited and must be amplified several times prior to microarray analysis (Yoon *et al.* 2004). For the samples collected by LCM, the random error from mRNA amplification and degradation during the staining could pose problems. In our study, the luminal epithelium at both implantation and inter-implantation sites was isolated by enzymatic digestion from over 100 mice and directly used for microarray analysis.

Because the uterus at implantation sites was used in previous microarray studies (Yoshioka *et al.* 2000, Reese *et al.* 2001), it was difficult to compare our data with theirs. In the study by Yoon *et al.* (2004), the luminal epithelium isolated by LCM was used for microarray analysis, and only three identical upregulated genes were detected both by us and by Yoon *et al.* (2004). Compared with inter-implantation sites, *Ggh*, inhibitor of DNA-binding 3, and secreted acidic cysteine-rich glycoprotein (*Sparc*) were increased by 2·44-, 3·33-, and 3·08-folds in our study, but by 1·63-, 1·89-, and 1·48-folds, by Yoon *et al.* (2004) respectively. Except for these three genes, other up- or downregulated genes were not shared. The main reason for these differences could be due to the methods for isolating luminal epithelium. We isolated the whole luminal epithelium at implantation or inter-implantation sites by enzymatic digestion, whereas Yoon *et al.* (2004) collected only the luminal epithelium immediately surrounding the implanting blastocyst. The luminal epithelium immediately surrounding the implanting blastocyst differed greatly from the rest of luminal epithelium in its gene

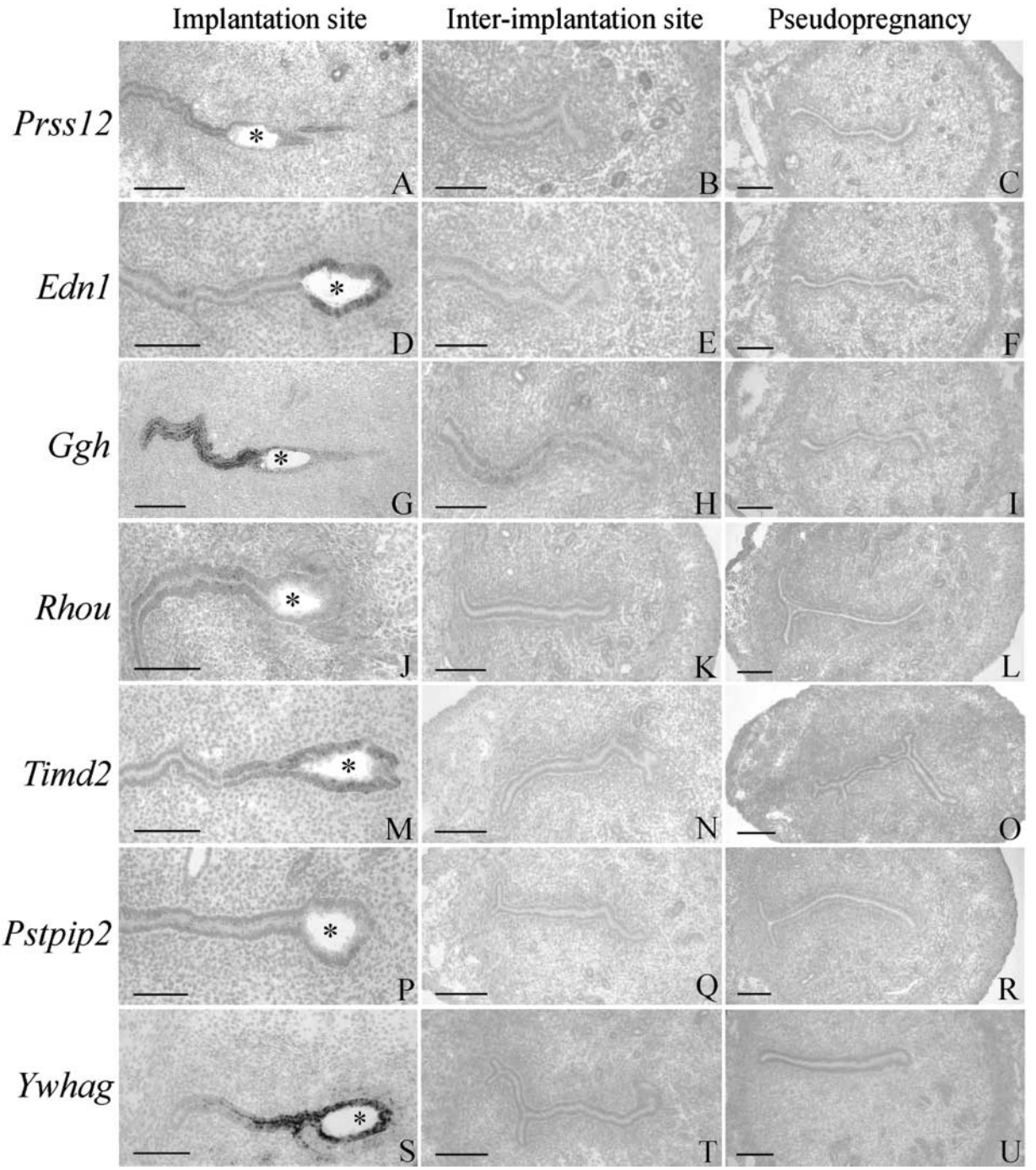

Figure 3 Confirmation by *in situ* hybridization, showing the expression pattern of protease, serine, 12 neurotrypsin, endothelin-1, γ-glutamyl hydrolase, Ras homolog gene family, member U, T-cell immunoglobulin and mucin domain containing 2, proline–serine–threonine phosphatase-interacting protein 2, and 3-monooxgenase/tryptophan 5-monooxgenase-activation protein, γ-polypeptide in mouse uteri at implantation site and inter-implantation site on day 5 of pregnancy, and on day 5 of pseudopregnancy respectively. Compared to inter-implantation site, the expression level of these seven genes in luminal epithelium was stronger at implantation site. On day 5 of pseudopregnancy, there were no detectable signals for these seven genes. *Implanting blastocyst; bar = 60 μm.

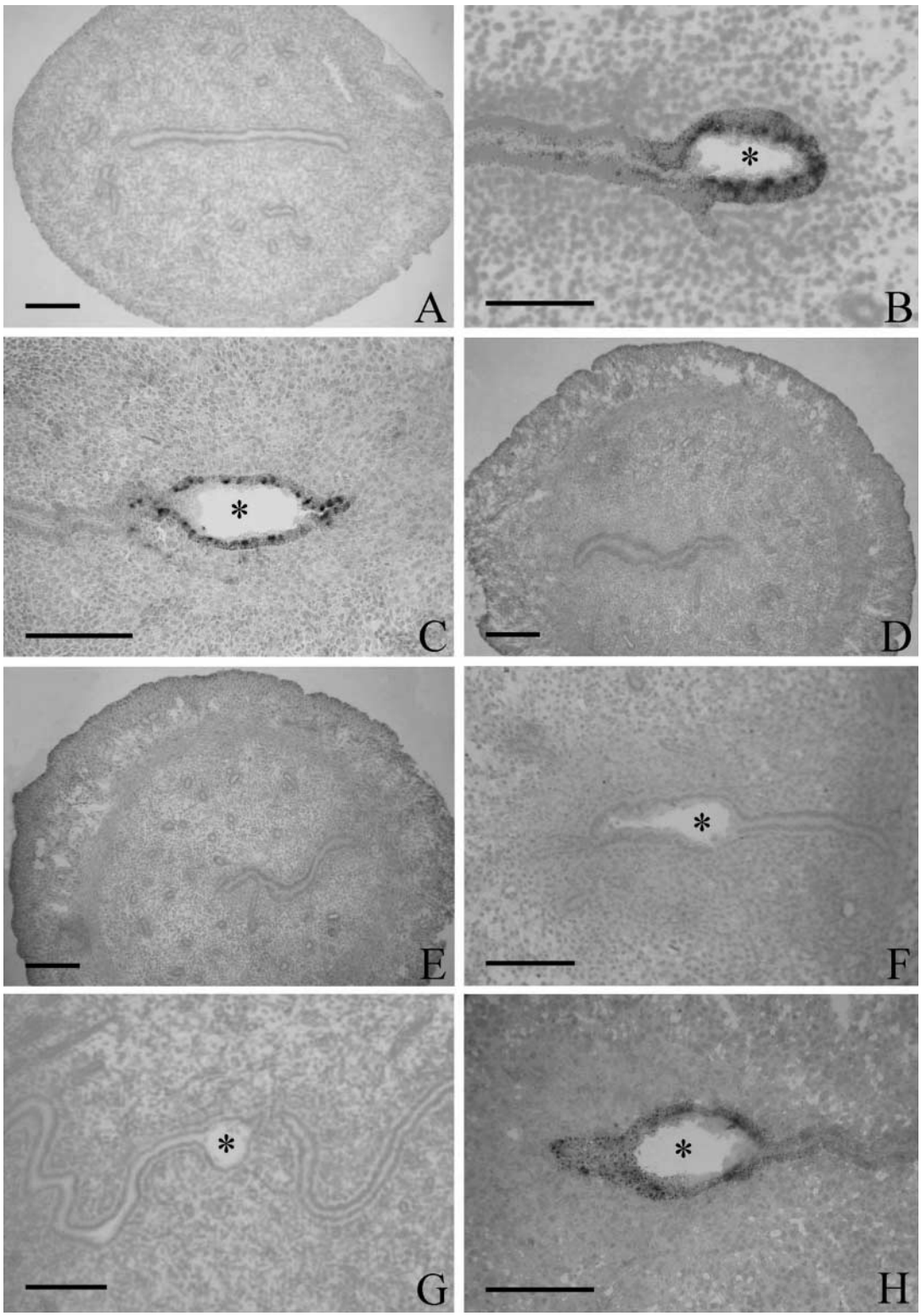

Figure 4 Cysteine rich protein 61 expression at implantation site. (A) Day 4 (0800 h); (B) day 4 (2400 h); (C) day 5 at implantation site; (D) day 5 at inter-implantation site; (E) day 5 of pseudopregnancy; (F) day 5 at implantation site (sense probe for control); (G) delayed implantation; (H) activation of delayed implantation. *Embryo; bar = 60 μm.

expression. For example, cyclooxygenase-2 and basigin were specifically expressed in the luminal epithelium surrounding the implanting blastocyst (Lim *et al.* 1997, Xiao *et al.* 2002).

Upregulated genes

In this study, 136 genes were upregulated by at least twofold, of which 24 were upregulated by at least threefold. *Prss12* was the highest one upregulated by 6·75-fold and was strongly expressed in the glandular epithelium and the luminal epithelium near the blastocyst at implantation site on day 5 of pregnancy, but not detected in the inter-implantation site on day 5 of pregnancy, and in the day 5 pseudopregnant uterus. It seems that *Prss12* in the luminal epithelium was specifically induced by implanting blastocyst. *Prss12*, also called motopsin, was highly expressed in mouse brain (Iijima *et al.* 1999). However, the expression, regulation, and function of this gene in early pregnancy still remain unknown.

Edn1 and *Ywhag* were strongly expressed in the luminal epithelium surrounding the implanting blastocyst, suggesting a role during embryo apposition and attachment. *Edn1* stimulates neutrophil adhesion to endothelial cells by an effect on the expression of adhesive molecules on the neutrophil surface. *Edn1* also stimulates neutrophil accumulation *in vivo* and *in vitro* in the heart (Lopez Farre *et al.* 1993). *Edn1* induces leukocyte rolling and adherence through a predominantly endothelin receptor A-mediated mechanism in the submucosal venules of the intestinal microcirculation (Boros *et al.* 1998). Human decidual cells in early pregnancy can synthesize and release EDN1. These cells also possess specific functional receptors for EDN1, which are coupled to phosphoinositide hydrolysis, suggesting a possible role for EDN1 in autocrine and/or paracrine function in human decidual cells (Kubota *et al.* 1992). *Ywhag*, also called 14-3-3 γ, is a member of the 14-3-3 family. The 14-3-3 family is a large group of highly conserved 30 kDa acidic proteins (Takahashi 2003). 14-3-3 proteins participate in integrin-activated signaling pathways through their interaction with docking protein p130 (Cas), which may contribute to important biological responses regulated by cell adhesion to the extracellular matrix (Garcia–Guzman *et al.* 1999). 14-3-3 ζ can regulate cell adhesion and spreading through the interaction with ADAM22 (Zhu *et al.* 2005). Whether *Ywhag* is involved in cell adhesion still remains unknown.

Timd2 was also highly expressed in the luminal epithelium surrounding the implanting blastocyst. However, there are no papers that mention its role in cell adhesion. The T-cell Ig and mucin domain-containing gene locus has been linked to differences in T(h)2 responsiveness and asthma susceptibility in mice (Encinas *et al.* 2005). *Timd2* is expressed preferentially in differentiated Th2 cells and is critical for the regulation of Th2 responses during autoimmune inflammation (Chakravarti *et al.* 2005). In normal pregnancy, particularly at the maternal–fetal interface, anti-inflammatory, Th-2, cytokines predominate (Wegmann *et al.* 1993). An appropriate balance between pro- and anti-inflammatory cytokines is thought to be crucial for determining the success or failure of a pregnancy (Formby 1995).

Rhou belongs to Ras homolog gene family. Ras homolog gene family, member I (ARHI) was downregulated in uterine serous papillary cancer compared with normal endometrial cells (Santin *et al.* 2005). Ras homolog gene family plays a central role in a wide range of physiological processes, including cell morphology, cell adhesion, cytokinesis, cell motility, and cell growth (Van Aelst & D'Souza-Schorey 1997, Hall 1998). However, the expression and function of *Rhou* during early pregnancy still remain to be determined.

Pstpip2, also called macrophage actin-associated tyrosine-phosphorylated protein (MAYP), directly regulates F-actin bundling and enhances filopodia formation and motility in macrophages. Filopodia are postulated to increase directional motility by acting as environmental sensors. The MAYP-stimulated increase in directional movement may be at least partly explained by enhancement of filopodia formation (Chitu *et al.* 2005). In our study, *Pstpip2* was expressed in all luminal epithelium at the implantation site, but not in the inter-implantation site on day 5 of pregnancy, and in the uterus on day 5 of pseudopregnancy, suggesting that *Pstpip2* may be involved in embryo apposition and attachment.

Downregulated genes

In our microarray, 223 genes were downregulated by at least twofold in the luminal epithelium at implantation site, of which nine were decreased by over threefold, including *N*-acetylneuraminate pyruvate lyase (5·26-fold), calbindin-28K (4·57-fold), brain acyl-CoA hydrolase (4·35-fold), glutathione S-transferase μ 1 (4·10-fold), solute carrier family 6 (3·85-fold), myeloid differentiation primary response gene 88 (3·61-fold), interleukin 1 receptor type 1 (3·38-fold), neuronal differentiation related protein (3·14-fold), and peripheral myelin protein 22 (3·08-fold). Although *N*-acetylneuraminate pyruvate lyase was greatly reduced at implantation sites, the expression and regulation of this gene is still unknown.

Calbindin-28K was decreased by 4·57-fold at implantation sites in our study. A previous study showed that calbindin-28K protein was increased in the endometrial epithelium just before implantation, but

disappeared at implantation sites after attachment (Luu *et al.* 2004). Because calbindin-28K is able to inhibit apoptosis in osteoblastic cells (Bellido *et al.* 2000), the apoptosis caused by the downregulation of calbindin-28K could destabilize the luminal epithelium at the implantation site and facilitate trophoblast invasion (Luu *et al.* 2004). However, calbindin-28K-deficient mice do not show implantation failure (Airaksinen *et al.* 1997). Calbindin-9K mRNA was also specifically downregulated at the implantation site (Nie *et al.* 2000). Although calbindin-28K-deficient mice are fertile, embryo implantation is blocked if both calbindin-9K and calbindin-28K are inhibited just before implantation (Luu *et al.* 2004).

A role for *Cyr61* in mediating embryo attachment at the implantation site

Cyr61 is also known as CCN1 (CCN is the initial of *Cyr61*, *Ctgf*, and NOV) and belongs to the CCN family. Other members of the CCN family include CCN2 (*Ctgf*), CCN3 (NOV), and the Wnt-inducible secreted proteins CCN4 (WISP-1), CCN5 (WISP-2), and CCN6 (WISP-3, Perbal 2001). *Cyr61* overexpression in the undifferentiated AN3CA endometrial cancer cell line led to decreased cell growth and increased apoptosis in liquid culture. Moreover, the increased apoptosis in these endometrial cancer cells with *Cyr61* over expression was associated with elevated expression of the pro-apoptotic proteins Bax, Bad, and tumor necrosis factor receptor-associated ligand (Chien *et al.* 2004). In the mouse, uterine epithelial cells surrounding the implanted embryo will undergo apoptotic cell death on day 5 evening or day 6 of pregnancy (Parr *et al.* 1987, Joswig *et al.* 2003). It is possible that the *Cyr61* expression might be closely related to subsequent apoptosis in the luminal epithelium.

We found that *Cyr61* was upregulated by 3·77-fold in the luminal epithelium at implantation sites. Because *Cyr61* was specifically induced in the luminal epithelium at the implantation site by the activated blastocyst, it may play a key role during embryo attachment. *Cyr61* and *Ctgf* supported the attachment of endothelial cells through integrin αvβ3 (Kireeva *et al.* 1998) and cell surface heparan sulfate proteoglycans (Chen *et al.* 2000, 2004). Integrin αvβ3 was expressed in the apical pole of the uterine luminal epithelium and on the epithelial surface of blastocyst (Aplin *et al.* 1996, Lessey *et al.* 1996). Nevertheless, the normal Mendelian ratio of *Cyr61* mutant embryos at E9.5 suggests that Cyr61 is not critical for implantation (Mo *et al.* 2002). It is possible that Cyr61 function may be compensated by other CCN members. CTGF shared many common functions with Cyr61, including promoting endothelial cell growth, migration, adhesion, and survival (Brigstock *et al.* 2002). Moreover, CTGF was also expressed in the luminal epithelium at mouse implantation site (Surveyor *et al.* 1998). In the *Ptgs2* null CD-1 mice, *Ptgs1* is upregulated and can maintain mouse implantation although cyclooxygenase (COX)-2 is essential for mouse implantation (Wang *et al.* 2004). However, whether CTGF is upregulated in *Cyr61* null mice remains to be determined.

In human endometrium, *Cyr61* was more highly expressed during the proliferative than during the secretory phase in endometrium (Punyadeera *et al.* 2005). *Cyr61* was one of the most upregulated genes in endometria of women with endometriosis and in ectopic endometrium (Absenger *et al.* 2004). Basic fibroblast growth factor, epidermal growth factor, tumor necrosis factor α, and interleukin-1 could stimulate *Cyr61* expression (Schutze *et al.* 1998). Furthermore, *Cyr61* could upregulate the synthesis of vascular endothelial growth factor (VEGF)-A and VEGF-C to regulate the processes of angiogenesis, inflammation, and matrix remodeling in the context of cutaneous wound healing (Chen *et al.* 2001, Brigstock 2002). Interestingly, *Cyr61* mutation led to impaired *Vegf-C* expression in the allantoic mesoderm, suggesting that *Cyr61*-regulated expression of *Vegf-C* plays a role in vessel bifurcation (Mo *et al.* 2002). VEGF was strongly expressed in mouse uterus during implantation period and played a key role in regulating vascular permeability and angiogenesis (Chakraborty *et al.* 1995, Halder *et al.* 2000). Increased vascular permeability and angiogenesis were crucial to successful implantation, decidualization, and placentation (Dey *et al.* 2004).

In conclusion, there are 136 genes upregulated and 223 genes downregulated in the luminal epithelium at the implantation site of mouse uterus by at least twofold in this microarray study compared to inter-implantation site. Among these regulated genes, there were 13 genes confirmed by RT-PCR and eight upregulated genes verified by *in situ* hybridization. *Cyr61* is specifically induced in the luminal epithelium at the implantation site by the activated blastocyst and may play a key role during embryo attachment. Our data could be a valuable source for future study on embryo implantation.

Acknowledgements

We thank Dr Sudhansu K Dey for helpful discussions and critical readings of the manuscript. We also thank Ren-Wei Su, Hao Yu, and Fei Gao for their help in collecting tissues and isolating luminal epithelium. This work was supported by Chinese National Natural Science Foundation grants 30330060, 30500361 and 30570198, and the Special Funds for Major State Basic Research Project (G1999055903). The authors declare that there is no conflict of interest that would prejudice the impartiality of this scientific work.

References

Absenger Y, Hess-Stumpp H, Kreft B, Kratzschmar J, Haendler B, Schutze N, Regidor PA & Winterhager E 2004 Cyr61, a deregulated gene in endometriosis. *Molecular Human Reproduction* **10** 399–407.

Airaksinen MS, Eilers J, Garaschuk O, Thoenen H, Konnerth A & Meyer M 1997 Ataxia and altered dendritic calcium signaling in mice carrying a targeted null mutation of the calbindin D28k gene. *PNAS* **94** 1488–1493.

Aplin JD, Spanswick C, Behzad F, Kimber SJ & Vicovac L 1996 Integrins β5, β3, αv are apically distributed in endometrial epithelium. *Molecular Human Reproduction* **2** 527–534.

Bellido T, Huening M, Raval-Pandya M, Manolagas SC & Christakos S 2000 Calbindin-D28k is expressed in osteoblastic cells and suppresses their apoptosis by inhibiting caspase-3 activity. *Journal of Biological Chemistry* **275** 26328–26332.

Bethin KE, Nagai Y, Sladek R, Asada M, Sadovsky Y, Hudson TJ & Muglia LJ 2003 Microarray analysis of uterine gene expression in mouse and human pregnancy. *Molecular Endocrinology* **17** 1454–1469.

Bigsby RM, Cooke PS & Cunha GR 1986 A simple efficient method for separating murine uterine epithelial and mesenchymal cells. *American Journal of Physiology* **251** E630–E636.

Boros M, Massberg S, Baranyi L, Okada H & Messmer K 1998 Endothelin 1 induces leukocyte adhesion in submucosal venules of the rat small intestine. *Gastroenterology* **114** 103–114.

Brigstock DR 2002 Regulation of angiogenesis and endothelial cell function by connective tissue growth factor (CTGF) and cysteine-rich 61 (CYR61). *Angiogenesis* **5** 153–165.

Carson DD, Bagchi I, Dey SK, Enders AC, Fazleabas AT, Lessey BA & Yoshinaga K 2000 Embryo implantation. *Developmental Biology* **223** 217–237.

Chakraborty I, Das SK & Dey SK 1995 Differential expression of vascular endothelial growth factor and its receptor mRNAs in the mouse uterus around the time of implantation. *Journal of Endocrinology* **147** 339–352.

Chakravarti S, Sabatos CA, Xiao S, Illes Z, Cha EK, Sobel RA, Zheng XX, Strom TB & Kuchroo VK 2005 Tim-2 regulates T helper type 2 responses and autoimmunity. *Journal of Experimental Medicine* **202** 437–444.

Chen N, Chen CC & Lau LF 2000 Adhesion of human skin fibroblasts to Cyr61 is mediated through integrin α6β1 and cell surface heparan sulfate proteoglycans. *Journal of Biological Chemistry* **275** 24953–24961.

Chen CC, Mo FE & Lau LF 2001 angiogenic factor Cyr61 activates a genetic program for wound healing in human skin fibroblasts. *Journal of Biological Chemistry* **276** 47329–47337.

Chen N, Leu SJ, Todorovic V, Lam SC & Lau LF 2004 Identification of a novel integrin alphavbeta3 binding site in CCN1 (CYR61) critical for pro-angiogenic activities in vascular endothelial cells. *Journal of Biological Chemistry* **279** 44166–44176.

Chien W, Kumagai T, Miller CW, Desmond JC, Frank JM, Said JW & Koeffler HP 2004 Cyr61 suppresses growth of human endometrial cancer cells. *Journal of Biological Chemistry* **279** 53087–53096.

Chitu V, Pixley FJ, Macaluso F, Larson DR, Condeelis J, Yeung YG & Stanley ER 2005 PCH family member MAYP/PSTPIP2 directly regulates F-actin bundling and enhances filopodia formation and motility in macrophages. *Molecular Biology of the Cell* **16** 2947–2959.

Dey SK, Lim H, Das SK, Reese J, Paria BC, Daikoku T & Wang H 2004 Molecular cues to implantation. *Endocrine Reviews* **25** 341–373.

Edwards RG 1995 Clinical approaches to increasing uterine receptivity during human implantation. *Human Reproduction* **10** (suppl 2) 60–66.

Encinas JA, Janssen EM, Weiner DB, Calarota SA, Nieto D, Moll T, Carlo DJ & Moss RB 2005 Anti-T-cell Ig and mucin domain-containing protein 1 antibody decreases TH2 airway inflammation in a mouse model of asthma. *Journal of Allergy and Clinical Immunology* **116** 1343–1349.

Finn CA & Porter DG 1975 *The uterus: cells and tissues of the endometrium.* Acton, MA: Publishing Sciences Group, Inc.

Formby B 1995 Immunologic response in pregnancy. Its role in endocrine disorders of pregnancy and influence on the course of maternal autoimmune diseases. *Endocrinology and Metabolism Clinics of North America* **24** 187–205.

Garcia-Guzman M, Dolfi F, Russello M & Vuori K 1999 Cell adhesion regulates the interaction between the docking protein p130(Cas) and the 14-3-3 proteins. *Journal of Biological Chemistry* **274** 5762–5768.

Halder JB, Zhao X, Soker S, Paria BC, Klagsbrun M, Das SK & Dey SK 2000 Differential expression of VEGF isoforms and VEGF(164)-specific receptor neuropilin-1 in the mouse uterus suggests a role for VEGF(164) in vascular permeability and angiogenesis during implantation. *Genesis* **26** 213–224.

Hall A 1998 Rho GTPases and the actin cytoskeleton. *Science* **279** 509–514.

He P, Varticovski L, Bowman ED, Fukuoka J, Welsh JA, Miura K, Jen J, Gabrielson E, Brambilla E, Travis WD *et al.* 2004 Identification of carboxypeptidase E and gamma-glutamyl hydrolase as biomarkers for pulmonary neuroendocrine tumors by cDNA microarray. *Human Pathology* **35** 1196–1209.

Herrler A, Von Rango U & Beier HM 2003 Embryo-maternal signalling: how the embryo starts talking to its mother to accomplish implantation. *Reproductive Biomedecine Online* **6** 244–256.

Iijima N, Tanaka M, Mitsui S, Yamamura Y, Yamaguchi N & Ibata Y 1999 Expression of a serine protease (motopsin PRSS12) mRNA in the mouse brain: *in situ* hybridization histochemical study. *Brain Research. Molecular Brain Research* **66** 141–149.

Joswig A, Gabriel HD, Kibschull M & Winterhager E 2003 Apoptosis in uterine epithelium and decidua in response to implantation: evidence for two different pathways. *Reproductive Biology and Endocrinology* **1** 44.

Kimber SJ & Spanswick C 2000 Blastocyst implantation: the adhesion cascade. *Seminar on Cell and Developmental Biology* **11** 77–92.

Kireeva ML, Lam SC & Lau LF 1998 Adhesion of human umbilical vein endothelial cells to the immediate-early gene product Cyr61 is mediated through integrin αvβ3. *Journal of Biological Chemistry* **273** 3090–3096.

Kubota T, Kamada S, Hirata Y, Eguchi S, Imai T, Marumo F & Aso T 1992 Synthesis and release of endothelin-1 by human decidual cells. *Journal of Clinical Endocrinology and Metabolism* **75** 1230–1234.

Lessey BA, Ilesanmi AO, Lessey MA, Riben M, Harris JE & Chwalisz K 1996 Luminal and glandular endometrial epithelium express integrins differentially throughout the menstrual cycle: implications for implantation, contraception, and infertility. *American Journal of Reproductive Immunology* **35** 195–204.

Lim H, Paria BC, Das SK, Dinchuk JE, Langenbach R, Trzaskos JM & Dey SK 1997 Multiple female reproductive failures in cyclo-oxygenase 2-deficient mice. *Cell* **91** 197–208.

Lopez Farre A, Riesco A, Espinosa G, Digiuni E, Cernadas MR, Alvarez V, Monton M, Rivas F, Gallego MJ, Egido J *et al.* 1993 Effect of endothelin-1 on neutrophil adhesion to endothelial heart. *Circulation* **88** 1166–1171.

Luu KC, Nie GY & Salamonsen LA 2004 Endometrial calbindins are critical for embryo implantation: evidence from *in vivo* use of morpholino antisense oligonucleotides. *PNAS* **101** 8028–8033.

Mo FE, Muntean AG, Chen CC, Stolz DB, Watkins SC & Lau LF 2002 CYR61 (CCN1) is essential for placental development and vascular integrity. *Molecular and Cellular Biology* **22** 8709–8720.

Ni H, Sun T, Ding NZ, Ma XH & Yang ZM 2002 Differential expression of microsomal PGE synthase at the implantation sites and in the decidual cells in mouse uterus. *Biology of Reproduction* **67** 351–358.

Nie GY, Li Y, Wang J, Minoura H, Findlay JK & Salamonsen LA 2000 Complex regulation of calcium-binding protein D9k (calbindin-D(9k)) in the mouse uterus during early pregnancy and at the site of embryo implantation. *Biology of Reproduction* **62** 27–36.

Parr EL, Tung HN & Parr MB 1987 Apoptosis as the mode of uterine epithelial cell death during embryo implantation in mice and rats. *Biology of Reproduction* **36** 211–225.

Perbal B 2001 NOV (nephroblastoma overexpressed) and the CCN family of genes: structural and functional issues. *Molecular Pathology* **54** 57–79.

Psychoyos A 1986 Uterine receptivity for implantation. *Annals of the New York Academy of Sciences* **476** 36–42.

Punyadeera C, Dassen H, Klomp J, Dunselman G, Kamps R, Dijcks F, Ederveen A, de Goeij A & Groothuis P 2005 Oestrogen-modulated gene expression in the human endometrium. *Cellular and Molecular Life Sciences* **62** 239–250.

Reese J, Das SK, Paria BC, Lim H, Song H, Matsumoto H, Knudtson KL, DuBois RN & Dey SK 2001 Global gene expression analysis to identify molecular markers of uterine receptivity and embryo implantation. *Journal of Biological Chemistry* **276** 44137–44145.

Rubanyi GM & Polakoff A 1994 Endothelins: molecular biology, biochemistry, pharmacology, physiology and pathophysiology. *Pharmacological Reviews* **46** 325–415.

Santin AD, Zhan F, Cane' S, Bellone S, Palmieri M, Thomas M, Burnett A, Roman JJ, Cannon MJ, Shaughnessy J Jr *et al.* 2005 Gene expression fingerprint of uterine serous papillary carcinoma: identification of novel molecular markers for uterine serous cancer diagnosis and therapy. *British Journal of Cancer* **92** 1561–1573.

Schutze N, Lechner A, Groll C, Siggelkow H, Hufner M, Kohrle J & Jakob F 1998 Human analog of murine cystein rich protein 61 is a 1α,25-dihydroxyvitamin D3 responsive immediate early gene in human fetal osteoblasts: regulation by cytokines, growth factors, and serum. *Endocrinology* **139** 1761–1770.

Spandorfer S & Rosenwaks Z 1999 Impact of maternal age and ovarian age on implantation efficacy. In *Embryo Implantation: Molecular, Cellular and Clinical Aspects*, pp 12–19. Ed DD Carson. New York: Springer-Verlag.

Surveyor GA, Wilson AK & Brigstock DR 1998 Localization of connective tissue growth factor during the period of embryo implantation in the mouse. *Biology of Reproduction* **59** 1207–1213.

Takahashi Y 2003 14-3-3 proteins: gene, gene expression, and function. *Neurochemical Research* **28** 1265–1273.

Tan Y, Li M, Cox S, Davis MK, Tawfik O, Paria BC & Das SK 2004 HB-EGF directs stromal cell polyploidy and decidualization via cyclin D3 during implantation. *Developmental Biology* **265** 181–195.

Van Aelst LV & D'Souza-Schorey C 1997 Rho GTPases and signal networks. *Genes and Development* **11** 2295–2322.

Wang H, Ma WG, Tejada L, Zhang H, Morrow JD, Das SK & Dey SK 2004 Rescue of female infertility from the loss of cyclooxygenase-2 by compensatory up-regulation of cyclooxygenase-1 is a function of genetic makeup. *Journal of Biological Chemistry* **279** 10649–10658.

Wegmann TG, Lin H, Guilbert L & Mosmann TR 1993 Bidirectional cytokine interactions in the maternal–fetal relationship: is successful pregnancy a TH2 phenomenon? *Immunology Today* **14** 353–356.

Xiao LJ, Chang H, Ding NZ, Ni H, Kadomatsu K & Yang ZM 2002 Basigin expression and hormonal regulation in mouse uterus during the peri-implantation period. *Molecular Reproduction and Development* **63** 47–54.

Yang YH, Dudoit S, Luu P, Lin DM, Peng V, Ngai J & Speed TP 2002 Normalization for cDNA microarray data: a robust composite method addressing single and multiple slide systematic variation. *Nucleic Acids Research* **30** e15.

Yoon SJ, Choi DH, Lee WS, Cha KY, Kim SN & Lee KA 2004 A molecular basis for embryo apposition at the luminal epithelium. *Molecular and Cellular Endocrinology* **219** 95–104.

Yoshioka K, Matsuda F, Takakura K & Noda Y 2000 Determination of genes involved in the process of implantation: application of GeneChip to scan 6500 genes. *Biochemistry and Biophysics Research Communication* **272** 531–538.

Zhu P, Sang Y, Xu H, Zhao J, Xu R, Sun Y, Xu T, Wang X, Chen L, Feng H, Li C & Zhao S 2005 ADAM22 plays an important role in cell adhesion and spreading with the assistance of 14-3-3. *Biochemistry and Biophysics Research Communication* **331** 938–946.

Zinaman MJ, Clegg ED, Brown CC, O'Connor J & Selevan SG 1996 Estimates of human fertility and pregnancy loss. *Fertility and Sterility* **65** 503–509.

Received in final form 21 May 2006
Accepted 5 June 2006